

## Accepted Manuscript

Syntheses, crystal structures, properties of metal coordination polymers based on a novel semi-rigid aromatic carboxylate ligand

Cui-Cui Wang, Gui-Mei Tang, Yong-Tao Wang, Jin-Hua Wang, Yue-Zhi Cui, Seik Weng Ng

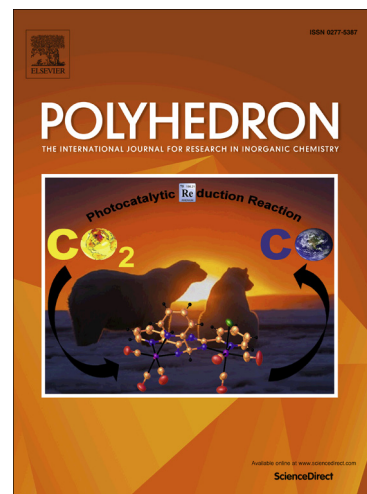
PII: S0277-5387(16)30659-3  
DOI: <http://dx.doi.org/10.1016/j.poly.2016.12.008>  
Reference: POLY 12366

To appear in: *Polyhedron*

Received Date: 21 October 2016  
Revised Date: 6 December 2016  
Accepted Date: 7 December 2016

Please cite this article as: C-C. Wang, G-M. Tang, Y-T. Wang, J-H. Wang, Y-Z. Cui, S. Weng Ng, Syntheses, crystal structures, properties of metal coordination polymers based on a novel semi-rigid aromatic carboxylate ligand, *Polyhedron* (2016), doi: <http://dx.doi.org/10.1016/j.poly.2016.12.008>

This is a PDF file of an unedited manuscript that has been accepted for publication. As a service to our customers we are providing this early version of the manuscript. The manuscript will undergo copyediting, typesetting, and review of the resulting proof before it is published in its final form. Please note that during the production process errors may be discovered which could affect the content, and all legal disclaimers that apply to the journal pertain.



**Syntheses, crystal structures, properties of metal coordination polymers based on a novel semi-rigid aromatic carboxylate ligand**

Cui-Cui Wang<sup>a</sup>, Gui-Mei Tang<sup>\*a</sup>, Yong-Tao Wang<sup>\*a</sup>, Jin-Hua Wang<sup>a</sup>, Yue-Zhi Cui<sup>a</sup> and Seik Weng Ng<sup>b</sup>

<sup>a</sup>*Department of Chemical Engineering, Shandong Provincial Key Laboratory of Fine Chemicals, Qilu University of Technology, Jinan, 250353, China*

<sup>b</sup>*Chemistry Department, Faculty of Science, King Abdulaziz University, Jeddah, Saudi Arabia*

\*Corresponding authors. E-mail: [ceswyt@qlu.edu.cn](mailto:ceswyt@qlu.edu.cn) (Y.-T. Wang); [meiguit@163.com](mailto:meiguit@163.com) (G.-M. Tang)

Fax: int code +86 0531 8963 1207. Tel: +86 0531 8963 1207.

**ABSTRACT**

A set of new metal coordination polymers constructed from a novel semi-rigid aromatic carboxylate ligand, namely,  $[M(L)(4PBI)(H_2O)]_n$  ( $M = Ni, Co$  and  $Cu$  for **1**, **2** and **3**, respectively) and  $[Cd(L)(4PBI)]_n$  (**4**) ( $H_2L = 3$ -(1-carboxyethyl) benzoic acid; **4PBI** = 2-(pyridin-4-yl)-(1*H*)-benzoimidazole), have been synthesized by the hydrothermal reaction, which were characterized by element analyses, FT-IR, UV-Vis diffuse reflection spectra, X-ray single-crystal diffraction, powder X-ray diffraction, and thermogravimetric analyses (TGA). Complexes **1**, **2** and **3** are iso-structural. They form a one-dimensional (1D) linear chain structure connected by semi-rigid aromatic anion and further assemble into a three-dimensional (3D) supramolecular framework by  $\pi \cdots \pi$  stacking and hydrogen bonding interactions. Complex **4** possesses two bi-nuclear units and displays two-dimensional (2D) layer which can further extend to a 3D supramolecular architecture *via* hydrogen bonding and weak packing interactions. Moreover, the luminescent property of complex **4** was investigated in the solid state at room temperature.

*Keywords:* hydrothermal reaction; 3-(1-carboxyethyl) benzoic acid; 2-(pyridin-4-yl)-(1*H*)-benzoimidazole; Crystal structures; Luminescence

ACCEPTED MANUSCRIPT

## 1. Introduction

During the past few decades, the rational design and construction of metal coordination polymers (**MCPs**) based on crystal engineering strategies have received great attention [1] because they possess novel structures and charming properties with potential applications in various areas such as photoluminescence [2], ion exchange [3], gas separation and storage [4], catalysis [5] and magnetism [6]. Typically, luminescent materials have been extensively explored for their diverse functionalities and application in sensing and optical device [7]. It is well known that the design and synthesis of **MCPs** with expected structures are still challenges for researchers. The syntheses of coordination polymers are mainly dependent on several factors such as centre metal ions [8] organic ligands [9], inorganic/organic anions [10], the ratios of metals and organic ligands [11], pH values [12], reaction temperature [13] and reaction time [14]. Among these, the organic ligands and centre metals play vital roles in the synthesis of **MCPs** [15]. Nevertheless, how to reasonably construct the expected architectures with unique properties is still a huge challenge. Selective design of organic ligands is usually crucial for the formation of these novel coordination frameworks [16]. Up to date, a variety of **MCPs** based on the multicarboxylates and flexible *N*-containing ligands have been constructed [17]. The aromatic multicarboxylate ligands have been intensely investigated due to their strong coordination ability and structure diversity [18]. However, the development and investigation of **MCPs** based on the semi-rigid aromatic carboxylate ligand still remain sparse. In this respect, we have designed one novel semi-rigid aromatic di-carboxylate ligand, 3-(1-carboxyethyl) benzoic acid (**H<sub>2</sub>L**) (Scheme 1), which display some specific features: i) the **H<sub>2</sub>L** ligand has two carboxylic groups that may be completely or partially deprotonated, including various coordination modes and allowing interesting structures; ii) The uncoordinated oxygen atoms act as acceptors in hydrogen bonding which can be advantageous to solidify the whole structures; iii) it can become in the formation of anion, which can make the final product become neutral structures and improve their thermal properties; iv) the existence of -CH- group can make one of carboxylate groups freely rotate in order to involve the coordination geometries of the specific metal ions, which can construct the specific structures of metal coordination polymers. Thus,

the exploring and design of the metal coordination polymers with the semi-rigid aromatic carboxylate ligand remain a challenge in field of MCPs, which will enrich and extend the content of the coordination chemistry and metal coordination polymers.

Additionally, the use of neutral auxiliary ligands such as *N*-donor ligands to the synthetic system of aromatic acids with metal ions is helpful to construct specific structures with interesting properties [19]. The ligand of 2-(pyridin-4-yl)-1*H*-benzoimidazole (**4PBI**) usually act as one of *N*-donor ligands. The **4PBI** ligand can adopt different conformations according to the geometric needs of different metal ions, and acts as donor and acceptor of hydrogen bondings [20]. Additionally, it can effectively improve the donated electron ability of benzoimidazole rings and makes it exhibit strong collaborative coordination ability with organic carboxylate ligands, which would be a powerful ligand for the construction of **MCPs** with diverse structures.

Herein, we would like to report the synthesis and characterization of four coordination polymers based on a semi-rigid aromatic bicarboxylate ligand and *N*-donor ligand, namely,  $[M(L)(\mathbf{4PBI})(H_2O)]_n$  ( $M = Ni, Co$  and  $Cu$  for **1**, **2** and **3**, respectively) and  $[Cd(L)(\mathbf{4PBI})]_n$  (**4**) ( $H_2L = 3$ -(1-carboxyethyl) benzoic acid; **4PBI** = 2-(pyridin-4-yl)-1*H*-benzoimidazole), which have been obtained under hydrothermal conditions. These **MCPs** have been characterized by FT-IR, UV-Vis spectra, single crystal X-ray diffraction, and powder X-ray diffraction. To the best of our knowledge, there is no report that **MCPs** containing this semi-rigid aromatic carboxylate ligand are synthesized and characterized. The thermogravimetric analyses (TGA) for complexes **1-4** were also discussed in details. Additionally, the fluorescence property of complex **4** was studied.

## 2. Experimental section

### 2.1. Materials and measurements

Sodium hydroxide was purchased from Tian Jin Guang Cheng Chemical Reagent Limited Corporation. 1,2-phenylene diamine was purchased from Sinopharm Chemical Reagent Limited Corporation. Nickel nitrate, Cobalt sulfate, Cadmium sulfate and Copper sulfate were obtained from Shanghai Chemical Reagent Corporation, Guang Zhou Chemical Reagent Factory, Shang Hai Chemical

Reagent Two Factory and Lai Yang Economic and Technological Development Zone Fine Chemical Factory, respectively. Polyphosphoric acid (PPA) was purchased from Aladdin Industrial Corporation. The ligand 3-(1-carboxyethyl) benzoic acid (**L**) and 2-(pyridin-4-yl)-(1H)-benzoimidazole (**4PBI**) were synthesized according to literature procedures [21] [22]. The reagents and solvents employed were used as received without further purification.

Elemental analyses were performed on an Elementar vario EL III microanalyser. The FT-IR spectra were recorded from KBr pellets in the range 400-4000  $\text{cm}^{-1}$  on a Bruker spectrometer. Powder X-ray diffraction (PXRD) was recorded on a Bruker D8 Advance diffractometer at 40 kV, 40 mA with a Cu-target tube and a graphite monochromator.  $2\theta$  falls in the range of 5-60°. The experimental PXRD patterns are in good agreement with the corresponding simulated ones except for the relative intensity variation because of the preferred orientations of the crystals. Therefore, the phase purity of the as-synthesized products is substantiated. UV-Vis spectra was recorded on a Shimadzu UV-2550 spectrometer. Diffuse reflectance UV-Vis spectra were recorded on a Shimadzu UV-2550 spectrometer equipped with an integrating sphere at room temperature in the range of 250-800 nm, in which barium sulfate ( $\text{BaSO}_4$ ) powder was used as a reference. Solid-state fluorescent studies were conducted on a HITACHI F-4500 system. Thermogravimetric analysis (TGA) data were collected with a TA SDT Q600 analyzer in  $\text{N}_2$  at a heating rate of 10  $^\circ\text{C min}^{-1}$  in the range of 20-900  $^\circ\text{C}$ .

### 2.2. Synthesis of 3-(1-carboxyethyl) benzoic acid ( $H_2L$ )

A mixture of 3-(1-cyanoethyl)benzoic acid (17.5 g, 0.1 mol), NaOH (10 g, 0.25 mol) and distilled water (100 mL) was refluxed on a steam bath for 7 h. After cooling to room temperature, the mixture was adjusted to pH 3 by the concentrated HCl solution. Subsequently, the mixture was allowed to cool to room temperature. Finally, the colorless crystal was collected by vacuum filtration. Yield (94.9%, 16.610 g). M.p. 158-160  $^\circ\text{C}$ . IR (KBr,  $\text{cm}^{-1}$ ): 2997(w), 2895(w), 1699(s), 1583(m), 1456(m), 1416(m), 1286(m), 1230(m), 1060(w), 937(br), 733(w), 686(w), 561(w).

### 2.3. Synthesis of 2-(pyridin-4-yl)-(1H)-benzoimidazole (**4PBI**)

Isonicotinic acid (1.477 g, 0.011 mol) and 1, 2-phenylene diamine (1.081 g, 0.010 mol) were mixed and grinded. To the reactions mixture, polyphosphoric acid (10 ml) was added. Subsequently, the reaction mixture was heated periodically under the irradiation of microwave. After the completed reaction, two blocks of ice were added to the mixture. When the reaction mixture was cooled to room temperature, pure water (30 ml) was poured to the mixture solution. The pH value of the solution was adjusted to 7 by adding the NaOH solution (10%). Finally, the solid product was collected and further crystallized from pure water to give a needle-like crystal. Yield (85.9%, 1.675 g). M.p. 226-228 °C. The microanalyses of compound **4PBI** are in good accordance with that reported previously [23].

#### 2.4. Synthesis of $[Ni(L)(4PBI)(H_2O)]_n$ (**1**)

A mixture of  $Ni(NO_3)_2 \cdot 6H_2O$  (0.0290 g, 0.1 mmol), **4PBI** (0.0195 g, 0.1 mmol), NaOH (0.0072 g, 0.18 mmol), **H<sub>2</sub>L** (0.0194 g, 0.1 mmol) and water (6 ml) were heated at 160 °C for 3 days in a 15 ml Teflon-lined vessel container. The reaction mixture was cooled to room temperature at a rate of 5 °C h<sup>-1</sup>. Green block crystals of complex **1** suitable for X-ray diffraction analysis were obtained (0.027 g, Yield: 58.18%) based on  $Ni(NO_3)_2$ . Elemental analysis calcd (%) for  $C_{22}H_{19}NiN_3O_5$  (464.10): C, 56.94; H, 4.13; N, 9.05; found: C, 56.81; H, 4.11; N, 9.01. IR (KBr, cm<sup>-1</sup>): 3067(w), 2970(w), 1616(m), 1597(m), 1564(s), 1531(s), 1447(s), 1406(s), 1317(m), 1282(m), 1238(w), 1126(w), 1061(w), 1022(m), 972(m), 916(m), 866(m), 847(w), 818(m), 788(w), 761(m), 743(s), 694(m), 640(w), 563(w), 516(w), 438(w).

#### 2.5. Synthesis of $[Co(L)(4PBI)(H_2O)]_n$ (**2**)

The preparation of complex **2** was similar to that **1** except that  $CoSO_4 \cdot 7H_2O$  (0.0280 g, 0.1 mmol) was instead of  $Ni(NO_3)_2 \cdot 6H_2O$ . The dark-red block crystals of complex **2** suitable for X-ray diffraction analysis were obtained (0.027 g, Yield: 58.14 %) based on  $CoSO_4$ . Elemental analysis calcd (%) for  $C_{22}H_{19}CoN_3O_5$  (464.34): C, 56.91; H, 4.12; N, 9.05; found: C, 56.86; H, 4.09; N, 9.05. IR (KBr, cm<sup>-1</sup>): 3065(w), 1614(m), 1541(m), 1437(m), 1400(s), 1315(m), 1281(w), 1227(w), 1142(w), 1105(w), 1063(w), 1018(w), 964(w), 837(w), 814(w), 748(s), 567(m), 520(w), 440(w), 407(w).

#### 2.6. Synthesis of $[Cu(L)(4PBI)(H_2O)]_n$ (**3**)

The synthesis preparation of complex **3** was similar to that of **1** except that  $\text{CuSO}_4 \cdot 5\text{H}_2\text{O}$  (0.0250 g, 0.1 mmol) was instead of  $\text{Ni}(\text{NO}_3)_2 \cdot 6\text{H}_2\text{O}$  and the mixture were heated at 120 °C. The dark-green block crystals of complex **3** suitable for X-ray diffraction analysis were obtained (0.025 g, Yield: 53.31%) based on  $\text{CuSO}_4$ . Elemental analysis calcd (%) for  $\text{C}_{22}\text{H}_{19}\text{CuN}_3\text{O}_5$  (468.96): C, 56.35; H, 4.08; N, 8.96; found: C, 56.19; H, 4.10; N, 8.93. IR (KBr,  $\text{cm}^{-1}$ ): 3063(w), 2972(w), 2758(w), 1620(s), 1593(m), 1528(s), 1452(s), 1435(m), 1406(s), 1319(m), 1288(m), 1240(w), 1128(w), 1076(w), 1060(w), 1028(w), 970(m), 914(w), 885(w), 841(w), 814(m), 785(w), 764(m), 748(s), 642(w), 565(w), 525(w), 444(w).

### 2.7. Synthesis of $[\text{Cd}(\text{L})(4\text{PBI})]_n$ (**4**)

The synthetic procedure for **4** was similar to that for **1** except that  $\text{CdSO}_4 \cdot 3/8 \text{H}_2\text{O}$  (0.026 g, 0.1 mmol) was instead of  $\text{Ni}(\text{NO}_3)_2 \cdot 6\text{H}_2\text{O}$ . The brown needle crystals of complex **4** suitable for X-ray diffraction analysis were obtained (0.042g, Yield: 84.03 %) based on  $\text{CdSO}_4$ . Elemental analysis calcd (%) for  $\text{C}_{22}\text{H}_{17}\text{CdN}_3\text{O}_4$  (499.81): C, 52.82; H, 3.40; N, 8.40; found: C, 52.95; H, 3.39; N, 8.43. IR (KBr,  $\text{cm}^{-1}$ ): 3414(br), 3061(w), 2963(w), 1620(s), 1566(s), 1539(s), 1445(s), 1400(s), 1384(s), 1323(m), 1283(w), 1240(m), 1072(w), 1014(w), 976(w), 910(w), 847(w), 818(m), 777(w), 748(s), 696(m), 660(w), 590(w), 559(w), 513(w), 432(w).

### 2.8. X-Ray crystallography

Single-crystal structure determinations of the ligand **4PBI** and four complexes were measured by an Agilent Technologies SuperNova Dual diffractometer equipped with graphite–monochromator Mo  $\text{K}\alpha$  radiation ( $\lambda = 0.71073 \text{ \AA}$ ). The lattice parameters were obtained by a least-squares refinement of the diffraction data. All the measured independent reflections were used in the structural analysis, and semi-empirical absorption corrections were applied using the CrysAlis PRO program [24]. The program SAINT was used for integration of the diffraction profiles [25]. The structure was solved by direct methods using the SHELXS program of the SHELXTL package and refined with SHELXL [26]. All non-hydrogen atoms were located in successive difference Fourier syntheses. The final refinement was performed by full-matrix least-squares methods with anisotropic thermal parameters for all the non-hydrogen atoms based on  $F^2$ . Except hydrogen atom bonded oxygen atom, the hydrogen atoms were

first found in difference electron density maps, and then placed in the calculated sites and included in the final refinement in the riding model approximation with displacement parameters derived from the parent atoms to which they were bonded. Special computations for the crystal structure discussions were carried out with PLATON for Windows [27]. A summary of the crystallographic data and structure refinements are listed in Table 2. Selected bond lengths and angles are given in Table 3. Corresponding hydrogen bonding data for **4PBI** and its complexes **1-4** are listed in Table 4.

### 3. Results and discussions

#### 3.1. FT-IR Spectra

The IR spectra of **H<sub>2</sub>L**, **4PBI**, and complexes **1-4** are shown in Fig. S1. The free ligand **H<sub>2</sub>L** exhibits wide peak characteristic  $\nu_{\text{OH}}$  stretching band at  $2986\text{ cm}^{-1}$ , while the  $\nu_{\text{OH}}$  stretching band of complexes **1-4** are observed at  $2970$ ,  $2976$ ,  $2972$  and  $2963\text{ cm}^{-1}$ , respectively. The strong peak at  $1691\text{ cm}^{-1}$  is ascribed to the  $-\text{COOH}$  functional groups for **H<sub>2</sub>L**. It is noteworthy that the carboxylate groups of **L** in complexes **1-4** are completely deprotonated because of the absence of the vibration band in the range of  $1760\text{-}1680\text{ cm}^{-1}$  attributed to the  $-\text{COOH}$  functional groups. The presence of characteristic bands is observed at  $1564$  and  $1406\text{ cm}^{-1}$ ,  $1541$  and  $1400\text{ cm}^{-1}$ ,  $1593$  and  $1406\text{ cm}^{-1}$ , and  $1539$  and  $1400\text{ cm}^{-1}$  for **1-4**, respectively, which may be attributed to the asymmetric and symmetric vibrations of the carboxylate groups. These results reveal that the O atoms of the carboxylate group are engaged in coordinating to the metal ions in these complexes. In addition, the moderate peaks at  $1605$ ,  $1589$  and  $1455\text{ cm}^{-1}$  suggest the existence of the frame vibration of benzene ring in free **H<sub>2</sub>L** ligand, and the moderate broad peak at  $943\text{ cm}^{-1}$  is attributed to  $\nu_{\text{O-H}}$  bending vibration of free **H<sub>2</sub>L** ligand. Additionally, the free ligand of **H<sub>2</sub>L** exhibit wide and loose peaks at nearly by  $2884\text{ cm}^{-1}$  characteristic  $\nu_{\text{C-H}}$  stretching band of  $-\text{CH}_3$  in **H<sub>2</sub>L** ligand and the moderate peak of  $753\text{ cm}^{-1}$  is ascribed to  $\delta_{\text{=CH}}$  bending vibration of **H<sub>2</sub>L** ligand.

For another free **4PBI** ligand, the characteristic  $\nu_{\text{N-H}}$  stretching band at  $3431\text{ cm}^{-1}$  and the weak peak at  $3055\text{ cm}^{-1}$  suggests that frame vibration of benzene ring in **4PBI** ligand. The strong peaks of  $1610$  and  $1436\text{ cm}^{-1}$  are ascribed to  $\nu_{\text{C=C}}$  and  $\nu_{\text{C=N}}$  vibration of benzimidazole in **4PBI** ligand,

respectively. The moderate peak at  $692\text{ cm}^{-1}$  is assigned to  $\nu_{\text{C-H}}$  stretching vibration of pyridine ring in **4PBI** ligand. In complexes **1-4**, it are observed at  $1616$  and  $761\text{ cm}^{-1}$  for **1**;  $1614$  and  $748\text{ cm}^{-1}$  for **2**;  $1620$  and  $748\text{ cm}^{-1}$  for **3**;  $1620$  and  $748\text{ cm}^{-1}$  for **4**, suggesting that there exists the formation of coordination from nitrogen atom of **4PBI**. In addition, the moderate peak at  $743\text{ cm}^{-1}$  is attributed to  $\delta_{\text{=CH}}$  bending vibration of benzene ring in **4PBI** ligand and the weak peak  $1112\text{ cm}^{-1}$  is attributed to  $\delta_{\text{C-H}}$  bending vibration of pyridine ring in **4PBI** ligand. The characteristics the stretching and bending vibration of the -OH groups of the water absorption bands at  $3067$ ,  $3065$  and  $3063\text{ cm}^{-1}$  for complexes **1-3**, respectively, providing the evidence for the coordinated water molecules.

### 3.2. UV-Vis absorbance and diffuse reflectance spectra

The UV-Vis spectra [28] of the free ligands **H<sub>2</sub>L** and **4PBI** in *N,N*-dimethylformamide (DMF) solution are presented in Table 1 and Fig. 2a. The UV-Vis spectrum of the free ligands **H<sub>2</sub>L** and **4PBI** exhibits one absorption peak at  $278$  and  $313\text{ nm}$ , respectively, which can be assigned to the  $\pi\text{-}\pi^*$  transition.

To evaluate the electronic absorbance feature of complexes **1-4**, the diffuse reflectance spectra were obtained using  $\text{BaSO}_4$  as standard at room temperature. The experimental results are depicted in Fig. 2b. Complexes **1-3** display obviously the absorbance bands in the uviolet to visible region; while there exist the bands only falling in the uviolet range for complex **4**. In the electronic spectra, all of complexes display the bands at the uviolet region, which are observed at  $263$  and  $321\text{ nm}$  for complex **1**,  $267$  and  $322$  for **2**,  $271$  and  $319\text{ nm}$  for **3**,  $271$  and  $320\text{ nm}$  for **4**, respectively. The bands at about  $270\text{ nm}$  can be assigned to the  $\pi\text{-}\pi^*$  transition of **L** ligand, while the UV bands found originating in the  $\pi\text{-}\pi^*$  transition of the **4PBI** are observed in the expected positions at about  $320\text{ nm}$ .

As illustrated in Fig. 2b, for complex **1**, one broad band falling in the visible region in the electronic spectra are observed at  $552\text{ nm}$ , which can be attributed to the  $[^3A_{2g} \rightarrow ^3T_{1g}(F)]$  transition [29]. The spectrum of complex **2** exhibits a broad band at  $623\text{ nm}$  that have intensities consistent with spin-allowed  $d\text{-}d$  transitions, which may be tentatively assigned to the transition of  $[^4T_{1g}(F) \rightarrow ^4T_{1g}(P)]$  [30]. On the basis of diffuse reflection spectrum of complex **3**, distorted octahedral geometry around Cu(II)

ion is suggested. The spectrum shows a low intensity broad band at 523 nm which is ascribed to the [ ${}^2E_g \rightarrow {}^2T_{2g}(F)$ ] transition [31].

### 3.3. Structure description of complexes **1**, **2** and **3**

The single crystal X-ray structural analysis reveals that complexes **1-3** are a one-dimension (1D) polymer and crystallize in the form of the monoclinic space group  $P2_1/n$ , and they are isostructural structures. As a matter of convenience, complex **1** is employed as a representative structure to be described in details. As shown in Fig. 3a, the asymmetric unit contains one Ni (II) ion, one **4PBI** ligand, one **L** ligand, and one coordinated water molecule. The Ni(II) centre takes a distorted octahedral geometry via coordinating to one pyridine-yl nitrogen atom (N1) of one **4PBI** ligand, four carboxylic oxygen atoms (O1A, O2A, O3 and O4) of two **L** ligands plus one oxygen atom (O1W) of one coordinated water molecule. The Ni-O bond distances in **1** range from 2.0330(2)–2.1540(2) Å and the Ni-N bond distance is 2.0580(2) Å (Table 3). The average Ni-O distance is 2.0964 Å, which are slightly longer than the common Ni-O distance 2.06 Å, and is in agreement with those found in documents [32]. The Co-O bond distances in **2** fall in the range of 2.0450(2)–2.1957(18) Å and the Co-N bond length is 2.0990(2) Å. The average Co-O distance is 2.1286 Å and Co-N distance is 2.0990 Å, which is slightly longer than the common Co-O and Co-N distances of 1.9400 and 1.9600 Å, respectively. The Cu-O distances in **3** fall in the range of 1.9720(3)–2.4640(2) Å and the Cu-N distance is 1.9940(3) Å (Table 3). The average bond length of Cu-O is 2.1662 Å, which is in agreement with those found in literatures published previously [32]. As shown in Fig. 3b, each adjoining pair of Ni (II) ions is connected by **L** ligands to form a 1D chain along the crystallographic *b* axis.

The supramolecular structures mainly depend on three kinds of interactions: the coordination bonds, the strong hydrogen bonds, and packing interactions. The O–H $\cdots$ O intermolecular hydrogen bond is generated through the oxygen atoms from the coordinated water molecules and the carboxylic oxygen atoms from the **L** ligands. These bond lengths and angles are 1.92(3) Å and 168(3)° for **1**, 1.88(3) Å and 167(3)° for **2**, and 1.80(3) Å and 174(4)° for **3**, respectively, through which 1D polymeric

chains are extended to a two-dimensional (2D) supramolecular layer along the crystallographic  $c$  axis (Fig. 3c).

In an addition, there exist two kinds of O–H $\cdots$ N hydrogen bonds and three kinds of C–H $\cdots$ O hydrogen bonds in **1-3** (Fig. 3d and Table 4): (a) The O–H $\cdots$ N intermolecular hydrogen bonds occur between the oxygen atoms of the coordinated water molecules and the nitrogen atoms of the **4PBI** ligands. These bond lengths and bond angles are 1.88(2) Å and 170(4) $^\circ$  for **1**, 1.87(2) Å and 170(3) $^\circ$  for **2**, and 1.86(2) Å and 175(5) $^\circ$  for **3**, respectively. (b) The O–H $\cdots$ N intermolecular hydrogen bondings generate between the oxygen atoms from the **L** ligands and nitrogen atoms of the **4PBI** ligands. These bond lengths and bond angles are 1.84(2) Å and 170(4) $^\circ$  for **1**, 1.83(2) Å and 171(3) $^\circ$  for **2**, and 1.81(3) Å and 176(3) $^\circ$  for **3**, respectively. (c) The C–H $\cdots$ O intermolecular hydrogen bondings originate from the carbon atoms from the **4PBI** ligands and oxygen atoms of the **L** ligands. These bond lengths and bond angles is 2.35 Å and 125 $^\circ$  for **1**, and these bond lengths and bond angles fall in the range of are 2.40–2.54 Å and 126–160 $^\circ$  for **2**, and 2.48–2.54 Å and 130–160 $^\circ$  for **3**, respectively. (d) The C–H $\cdots$ O intermolecular hydrogen bondings construct between the carbon atoms from the **4PBI** ligands and oxygen atoms of the coordination water molecules. These bond lengths and bond angles are 2.60 Å and 156 $^\circ$  for **1**, 2.57 Å and 157 $^\circ$  for **2**, and 2.53 Å and 160 $^\circ$  for **3**, respectively. Furthermore, another type of C–H $\cdots$ O intermolecular hydrogen bond is generated through the oxygen atoms from **L** ligands and the carbon atoms from **L** ligands for **1**. These bond lengths and bond angles are 2.58 Å and 140 $^\circ$  for **1**. Apart from these hydrogen bonding interactions, it is worth noting that there exist two kinds of weak  $\pi\cdots\pi$  packing interactions between the aromatic rings. One occurs between the imidazole groups and phenyl ones (3.6010(17), 3.5843(16) and 3.636(2) Å for **1**, **2** and **3**, respectively) and the other do between two phenyl groups (3.6434(16), 3.6663(14) and 3.6183(17) Å for **1**, **2** and **3**, respectively). Additionally, another types of  $\pi\cdots\pi$  packing interactions are observed in **3** (Cg(2) $\cdots$ Cg(1)<sup>k</sup>, 2.6365(15) Å, <sup>k</sup> x, y, z; Cg(3) $\cdots$ Cg(1)<sup>l</sup>, 2.6365(15) Å, <sup>l</sup> -1/2+x, 1/2-y, -1/2+z). Finally, the 3D supramolecular framework is obtained by a variety of hydrogen bonds and  $\pi\cdots\pi$  stacking interactions (Fig.3d).

#### 3.4. Structure description of complex 4

The results of the X-ray crystallographic analysis illustrate that complex **4** is a 2D network and it crystallizes in the triclinic space group *P*-1. As depicted in Fig. 4a, the asymmetric unit of complex **4** is made of two unique cadmium ions, three **L** ligands and two **4PBI** ligands. The central Cd1 ion is seven coordinated by two nitrogen atoms of two different **4PBI** ligands and five oxygen atoms of three **L** ligands. Seven O-donor atoms from **L** ligands form at the base plane of the distorted pentagonal bipyramid, and the vertexes of the distorted pentagonal bipyramid are made of two nitrogen atoms from two **4PBI** ligands. The Cd1 center deviate from the base plane about 0.0500(2) Å. Similar to that of Cd1, Cd2 adopts distorted pentagonal bipyramid with five oxygen atoms of three **L** ligands and two nitrogen atoms of two different **4PBI** ligands. The base plane of the pentagonal bipyramid consists of seven oxygen atoms from three **L** ligands, and the apexes of bipyramid are occupied by two nitrogen atoms from two **4PBI** ligands. The central Cd2 ion is slightly from the base plane about 1.5566(3) Å. The bond distances of Cd-O and Cd-N fall in the range of 2.251(3)–2.481 Å and 2.318(4)–2.360(3) Å (Table 3), respectively, which are normal values in some documents [32]. The bond angles of O-Cd-O, O-Cd-N and N-Cd-N in range of are 54.26(8)–157.12(8)°, 82.19(11)–109.76(12)° and 163.86(12)–164.60(12)°, respectively. Interestingly, there are two kinds of coordination modes for **L** ligands: one ligand acts as a bi-dentate mode; another does as the mono-dentate mode. As a result, one binuclear Cd structure was formed (Fig. 4a). Two Cd centers (Cd1 and Cd2) are connected by one **4PBI** ligand and one **L** ligand (Fig. 4a). In other words, these binuclear units are further extended to a 2D layer through **4PBI** and **L** ligands (Fig. 4b).

Interestingly, it is observed that there exist four kinds of hydrogen bonds (Fig. 4c and Table 4): (a) The intermolecular hydrogen bonds of N–H···O (N(3)–H(3)···O(2)<sup>e</sup> 1.92 Å, <sup>e</sup>1-x, 2-y, -z; N(6)–H(6)···O(6)<sup>a</sup> 1.94 Å, <sup>a</sup>1-x, 1-y, 1-z) (Table 4) are generated through nitrogen atoms of **4PBI** ligand and oxygen atoms of **L** ligand. (b) The intermolecular hydrogen bondings of C–H···O (C(7)–H(7)···O(5)<sup>f</sup> 2.49 Å, <sup>f</sup>1-x, 2-y, 1-z; C(17)–H(17)···O(1)<sup>a</sup> 2.51 Å, <sup>a</sup>1-x, 1-y, 1-z.) are observed through carbon atoms of **L** ligand and oxygen atoms of **L** ligand. (c) The hydrogen bondings of C–H···O (C(21)–H(21)···O(8)<sup>a</sup> 2.45 Å, <sup>a</sup>1-x, 1-y, 1-z; C(24)–H(24)···O(2)<sup>f</sup> 2.57 Å, <sup>f</sup>1-x, 2-y, -z; C(33)–H(33)···O(3)<sup>f</sup> 2.42 Å, <sup>f</sup>1-x, 2-y, 1-z;

C(34)–H(34)⋯O(2)<sup>g</sup> 2.34 Å, <sup>g</sup>x, y, 1+z; C(36)–H(36)⋯O(6)<sup>a</sup> 2.58 Å, <sup>a</sup>1-x, 1-y, 1-z; C(22)–H(22)⋯O(6) 2.36 Å) occur from **L** ligand and carbon atoms of **4PBI** ligand.

Except from these hydrogen bonds, there exist weak C–H⋯ $\pi$  interactions between C13–H13F and the phenyl ring (C27–C32)<sup>j</sup> (<sup>j</sup>-x, 2-y, 1-z), where the distance of C–H⋯ $\pi$  is 3.450 Å and the angle is 124°. These supramolecular interactions extend the 2D supramolecular layers to a 3D supramolecular framework along the crystallographic *b* axis (Fig. 4c).

To investigate the topological structure of the complex **4**, the Cd(II) atoms can be regarded as five connecting nodes, whereas the **L**, **4PBI** ligands act as linear linker which bridges two adjacent Cd(II) atoms. Thus, the whole network is simplified to the (3,5), (4,5), (6,5) topological structure, which is same to those found in some 2D **MCPs** (Fig. 4d) [33]. Interestingly, the present topological network is non-uniform topological structure, which is obviously different from those documented in literatures [34].

### 3.5. Coordination modes of *L* in complexes 1-4

According to the structure descriptions mentioned above, we could find that the two carboxylate groups of **L** ligand exhibit two kinds of coordination modes (Scheme 2). In complexes **1-3**, **L** is completely deprotonated. The coordination modes of two carboxyl groups in **L** are same and display a  $\mu_2\text{-}\eta^1:\eta^1:\eta^1:\eta^1$  coordination mode (Scheme 2a), which coordinates with metal ions such as, Ni<sup>2+</sup>, Co<sup>2+</sup>, and Cu<sup>2+</sup> for **1-3**, respectively. However, in complex **4**, the **L** ligand is partially deprotonated, and the two carboxyl groups of **L** adopt the completely different coordination modes, that is,  $\mu_2\text{-}\eta^1:\eta^1:\eta^1:\eta^1$  (Scheme 2a) and  $\mu_3\text{-}\eta^1:\eta^1:\eta^2:\eta^1$  (Scheme 2b). From the viewpoint of the present results, it is obvious that the diverse coordination modes of carboxylate groups resulted in the structural differences of complexes **1-4**.

### 3.6. Effects of the central metals on the structures

As mentioned above, we could see that the central metal ions play important roles in the final structures of **1-4**. The difference coordination numbers of central metal ions are an important reason for the complex with different structural motifs. The coordination number (CN) of Cd ions in **4** (CN = 7) is

larger than that of Ni ions, Co ions and Cu ions in **1-3** (CN = 6), which may be attributed to the fact that the radius of Cd ions is larger than that of Ni ions, Co ions and Cu ions. Additionally, in complexes **1-3**, the coordination numbers around metal centers are uniform, which may be assigned to the similarity radius of Ni ions, Co ions and Cu ions. The present results provide us with the fact that suitable metal ions may be a good candidate for the construction of **MCPs** with diverse dimensionalities.

### 3.7. Effects of 4PBI ligands on the structures

Apart from the effects of the coordination modes for **L** and the metal ions, the **4PBI** ligand show different coordination modes in complexes **1-4**, respectively (Scheme 2c and 2d). As illustrated in Scheme 2c, in complexes **1-3**, there exists mono-dentate mode for 4PBI ligand. However, bis-dentate bridging mode of **4PBI** ligand is observed in complex **4** (Scheme 2d). The present results indicate that the **4PBI** ligands also significant effects on the formation of the final structures. For complexes **1-3**, they have a 1D chain. When the **4PBI** ligands were conducted to the reaction system of **1-3**, a 3D supramolecular framework network is found. Complex **4** exhibits a 2D layer structure. When the **4PBI** ligands were introduced into the reaction system of **4**, another 3D supramolecular architecture is observed. Obviously, the auxiliary ligands also play an important role in the construction of the final structures.

### 3.8. Powder X-ray diffraction (XRD)

To confirm the pure phase of these complexes, PXRD experiment has been carried out. As illustrated in Fig.5-8, the peak positions of the simulated and experimental PXRD patterns are in good accordance with each other, which illustrates the phase purity of the products [35].

### 3.9. Thermogravimetric analyses (TGA)

In order to characterize the compounds more fully in terms of thermal stability, the thermal behaviors of **1-4** were examined by TGA. As illustrated in Fig. 9-12, all of the TGA curves for **1-3** are similar. The TGA curves show that first weight loss occurs in the range of 29-164 °C (obsd 1%, calcd 3.9%) for **1**, 31-166 °C (obsd 1%, calcd 3.9%) for **2**, and 27-144 °C (obsd 1%, calcd 3.8%) for **3**, respectively, which corresponds to the loss of coordination water molecules. The present results indicate

that there exist strong hydrogen bonds among the water molecules. The framework starts to collapse in the temperature range of 247-800 °C (obsd 77%, calcd 78%) for **1**, 206-800 °C (obsd 60%, calcd 78.3%) for **2**, and 184-800 °C (obsd 75%, calcd 82%) for **3**, respectively, revealing the departure of organic ligands. The remaining weight is attributed to the final product of Ni<sub>2</sub>O<sub>3</sub> (obsd 22%, calcd 18%) for **1**, Co<sub>2</sub>O<sub>3</sub> (obsd 39%, calcd 17.8%) for **2**, and CuO (obsd 24%, calcd 17%) for **3**, respectively. The TGA curve of **4** reveals that first weight loss falls from 190 to 538 °C (obsd 97.5%, calcd 74.3%), showing the departure of organic ligands. Finally, the final residual can be assigned to the formation of CdO (obsd 25%, calcd 25.7%) for **4**.

### 3.10. Luminescent spectra

The luminescence properties of complexes containing d<sup>10</sup> metals have been intensely researched owing to their potential applications in photochemistry and sensors [36]. Therefore, in this paper, the photoluminescence properties of complex **4**, **L**, and **4PBI** were investigated in the solid state at room temperature. As shown in Fig. 13, the main emission peak of **L** is found at 414 nm ( $\lambda_{\text{ex}} = 286$  nm). In an addition, the two maximum emission peaks of **4PBI** are located at 411 nm and 516 nm ( $\lambda_{\text{ex}} = 280$  nm), respectively. The emission bands of these free ligands are probably caused by the  $\pi^* \rightarrow \pi$  or  $\pi^* \rightarrow n$  transitions [37]. Complex **4** displays emission band located at 459 nm with excitation at 317 nm. Compared with the emission spectrum of **L** and **4PBI** ligands, red-shifts of emission bands for **4** have been observed. Since the Cd<sup>2+</sup> ions are difficult to oxidize or to reduce due to their d<sup>10</sup> configuration, the emission of complex **4** is neither metal-to-ligand charge transfer (MLCT) nor ligand-to-metal charge transfer (LMCT) in nature [38]. The emission of the complex may be assigned to the intraligand fluorescence emission. The present results indicate that complex **4** can be one of promising candidates for luminescent materials.

## 4. Conclusions

In summary, we have successfully designed and developed a set of metal coordination polymers based on the semi-rigid aromatic carboxylate group, which display interesting structural motifs with different dimensionalities. The present results indicate that the metal centers and the bridging ligand play a key

role in final structures, which confirms the significant potential of constructing structures based on semi-rigid aromatic acid and *N*-donor ligands, and provides an animated example to construct novel metal coordination polymers. Furthermore, the fluorescent property of **4** makes it one of the promising candidates for photoluminescent material. Currently, the design and explore of other metal coordination polymers based on the semi-rigid aromatic carboxylate groups, which show the specific motifs and interesting properties, is on the way at our laboratory.

### Acknowledgements

This work was financially supported by the Project of Shandong Province Higher Educational Science and Technology Program (J09LB03), Shandong Distinguished Middle-aged Young Scientist Encouragement and Reward Foundation (BS2011CL034), and Program for Scientific Research Innovation Team in Colleges and Universities of Shandong Province. Prof. Yue-Zhi Cui gratefully thanks to the National Natural Science Foundation of China (No. 21276149).

### Appendix A. supplementary material

CCDC 994678-994681 contain the supplementary crystallographic data of the ligand and its complex for this article. These data can be obtained free of charge via [http://www.ccdc.cam.ac.uk/data\\_request/cif](http://www.ccdc.cam.ac.uk/data_request/cif), or from the Cambridge Crystallographic Data Centre, 12 Union Road, Cambridge CB2 1EZ, UK. Telephone: +44 01223 762910 Facsimile: +44 01223 336033; or e-mail: [deposit@ccdc.cam.ac.uk](mailto:deposit@ccdc.cam.ac.uk). Supplementary data associated with this article can be found, in the online version, at <http://dx.doi.org/10.1016>.

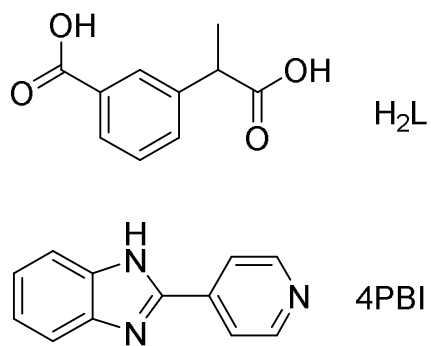
### References

- [1] (a) V. N. Vukotic, S. J. Loeb, *Chem. Soc. Rev.* 41 (2012) 5896; (b) O. M. Yaghi, M. O'Keeffe, N. W. Ockwig, H. K. Chae, M. Eddaoudi, J. Kim, *Nature* 423 (2003) 705; (c) J.-P. Zhang, Y.-B. Zhang, J.-B. Lin, X.-M. Chen, *Chem. Rev.* 112 (2012) 1001; (d) M. Li, D. Li, M. O'Keeffe, O. M. Yaghi, *Chem. Rev.* 114 (2014) 1343; (e) X. Kong, H. Deng, F. Yan, J. Kim, J. A. Swisher, B. Smit, O. M. Yaghi, J. A. Reimer, *Science* 341 (2013) 882.
- [2] (a) J. Heine, K. Muller-Buschbaum, *Chem. Soc. Rev.* 42 (2013) 9232; (b) M. D. Allendorf, C. A. Bauer, R. K. Bhakta, R. J. T. Houk, *Chem. Soc. Rev.* 38 (2009) 1330; (c) J. Rocha, L. D. Carlos, F. A. A. Paz, D. Ananias, *Chem. Soc. Rev.* 40 (2011) 926; (d) Y. Cui, Y. Yue, G. Qian, B. Chen, *Chem. Rev.* 112 (2012) 1126; (e) L. Zhou, J. Zhang, Y. Z. Li, H. B. Du, *CrystEngComm* 15

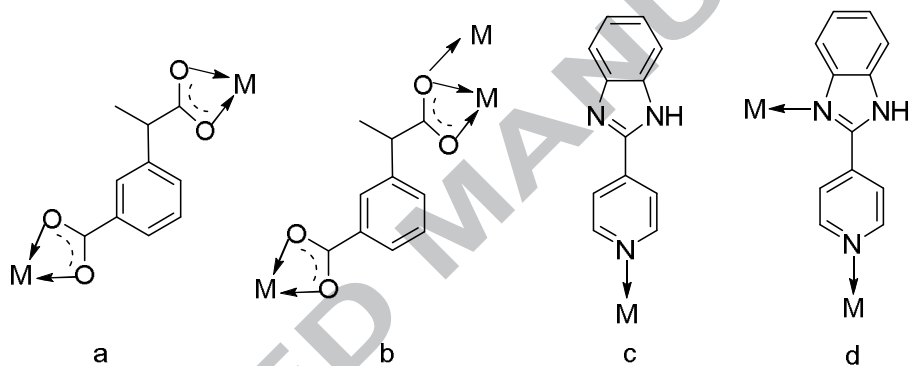
- (2013) 8989; (f) X. H. Chang, Y. Zhao, M. L. Han, L. F. Ma, L. Y. Wang, *CrystEngComm* 16 (2014) 6417.
- [3] (a) B. Manna, A. K. Chaudhari, B. Joarder, A. Karmakar, S. K. Ghosh, *Angew. Chem. Int. Ed.* 52 (2013) 998; (b) A. Aijaz, P. Lama, P. K. Bharadwaj, *Inorg. Chem.* 49 (2010) 5883; (c) L. Mi, H. Hou, Z. Song, H. Han, H. Xu, Y. Fan, S.-W. Ng, *Cryst. Growth Des.* 7 (2007) 2553.
- [4] (a) N. A. Ramsahye, G. Maurin, S. Bourrelly, P. L. Llewellyn, T. Devic, C. Serre, T. Loiseau, G. Ferey, *Adsorption* 13 (2007) 461; (b) M. Zhang, Z. J. Pu, X. L. Chen, X. L. Gong, A. X. Zhu, L. M. Yuan, *Chem. Commun. (Camb.)* 49 (2013) 5201; (c) S. J. Alesadi, F. Sabzi, *Int. J. Hydrogen Energy* 40 (2015) 1651; (d) K. Sumida, D. L. Rogow, J. A. Mason, T. M. McDonald, E. D. Bloch, Z. R. Herm, T.-H. Bae, J. R. Long, *Chem. Rev.* 112 (2012) 724; (e) J.-R. Li, J. Sculley, H.-C. Zhou, *Chem. Rev.* 112 (2012) 869; (f) H. Furukawa, K. E. Cordova, M. O'Keeffe, O. M. Yaghi, *Science* 341 (2013) 974; (g) B. Seoane, J. Coronas, I. Gascon, M. E. Benavides, O. Karvan, J. Caro, F. Kapteijn, J. Gascon, *Chem. Soc. Rev.* 44 (2015) 2421.
- [5] (a) J. W. Liu, L. F. Chen, H. Cui, J. Y. Zhang, L. Zhang, C. Y. Su, *Chem. Soc. Rev.* 43 (2014) 6011; (b) B. Gole, A. K. Bar, A. Mallick, R. Banerjee, P. S. Mukherjee, *Chem. Commun. (Camb.)* 49 (2013) 7439; (c) A. Dhakshinamoorthy, H. Garcia, *Chem. Soc. Rev.* 43 (2014) 5750; (d) M. Yoon, R. Srirambalaji, K. Kim, *Chem. Rev.* 112 (2012) 1196; (e) A. H. Chughtai, N. Ahmad, H. A. Younus, A. Laypkov, F. Verpoort, *Chem Soc Rev* 44 (2015) 6804; (f) L. Liu, Z.-B. Han, S.-M. Wang, D.-Q. Yuan, S. W. Ng, *Inorg. Chem.* 54 (2015) 3719; (g) Z. H. Xu, L. L. Han, G. L. Zhuang, J. Bai, D. Sun, *Inorg. Chem.* 54 (2015) 4737; (h) H. Zhang, J. H. Lv, K. Yu, C. M. Wang, C. X. Wang, D. Sun, B. B. Zhou, *Dalton Trans.* 44 (2015) 12839; (i) J.-H. Wang, G.-M. Tang, Y.-T. Wang, Y.-Z. Cui, J.-J. Wang, S. W. Ng, *Dalton Trans.* 44 (2015) 17829; (j) J.-H. Wang, E. Zhang, G.-M. Tang, Y.-T. Wang, Y.-Z. Cui, S. W. Ng, *J. Solid State Chem.* 241 (2016) 86.
- [6] (a) E. Coronado, G. Minguez Espallargas, *Chem. Soc. Rev.* 42 (2013) 1525; (b) M. Kurmoo, *Chem Soc Rev* 38 (2009) 1353; (c) C. W. Ingram, L. Liao, J. Bacsá, I. Harruna, D. Sabo, Z. J. Zhang, *Cryst. Growth Des.* 13 (2013) 1131; (d) G. W. Xu, Z. L. Wang, G. X. Wen, S. S. Guo, D. S. Li, J. Zhang, *Inorg. Chem. Commun.* 55 (2015) 17; (e) M.-H. Zeng, Z. Yin, Y.-X. Tan, W.-X. Zhang, Y.-P. He, M. Kurmoo, *J. Am. Chem. Soc.* 136 (2014) 4680; (f) C.-F. Wang, R.-F. Li, X.-Y. Chen, R.-J. Wei, L.-S. Zheng, J. Tao, *Angew. Chem. Int. Ed.* 54 (2015) 1574.
- [7] (a) S. J. Liu, Y. B. Huang, Z. J. Lin, X. F. Li, R. Cao, *RSC Advances* 3 (2013) 9279; (b) X. Z. Song, S. Y. Song, C. Qin, S. Q. Su, S. N. Zhao, M. Zhu, Z. M. Hao, H. J. Zhang, *Cryst. Growth Des.* 12 (2012) 253; (c) L. E. Kreno, K. Leong, O. K. Farha, M. Allendorf, R. P. Van Duyne, J. T. Hupp, *Chem. Rev.* 112 (2012) 1105; (d) A. Ramdass, V. Sathish, M. Velayudham, P. Thanasekaran, S. Umopathy, S. Rajagopal, *RSC Adv.* 5 (2015) 38479.
- [8] (a) H. L. Jiang, B. Liu, Q. Xu, *Cryst. Growth Des.* 10 (2010) 806; (b) Y. Yang, J. Yang, P. Du, Y. Y. Liu, J. F. Ma, *CrystEngComm* 16 (2014) 1136; (c) L. L. Wen, F. M. Wang, X. K. Leng, M. M. Wang, Q. J. Meng, H. Z. Zhu, *J. Inorg. Organomet. Polym.* 20 (2010) 313; (d) Y.-T. Wang, G.-M. Tang, W.-Z. Wan, Y. Wu, T.-C. Tian, J.-H. Wang, C. He, X.-F. Long, J.-J. Wang, S. W. Ng, *CrystEngComm* (2012) 3802; (e) Y.-T. Wang, S.-C. Yan, G.-M. Tang, C. Zhao, T.-D. Li, Y.-Z. Cui, *Inorg. Chim. Acta* 376 (2011) 492; (f) Y. T. Wang, G. M. Tang, Y. Wu, X. Y. Qin, D. W. Qin, *J. Mol. Struct.* 831 (2007) 61.
- [9] (a) A. Y. Robin, K. M. Fromm, *Coord. Chem. Rev.* 250 (2006) 2127; (b) Y. T. Wang, G. M. Tang, Y. Q. Wei, T. X. Qin, T. D. Li, J. B. Ling, X. F. Long, *Inorg. Chem. Commun.* 12 (2009) 1164; (c) Y. T. Wang, G. M. Tang, T. D. Li, J. C. Yu, Y. Q. Wei, J. B. Ling, X. F. Long, *Aust. J. Chem.* 63 (2010) 336.
- [10] (a) H. Wang, D. Zhang, D. Sun, Y. Chen, L.-F. Zhang, L. Tian, J. Jiang, Z.-H. Ni, *Cryst. Growth Des.* 9 (2009) 5273; (b) H. Y. Bai, J. F. Ma, J. Yang, Y. Y. Liu, W. Hua, J. C. Ma, *Cryst. Growth Des.* 10 (2010) 995; (c) R.-J. Wei, J. Tao, R.-B. Huang, L.-S. Zheng, *Eur. J. Inorg. Chem.* (2013) 916.
- [11] X. H. Bu, W. Chen, W. F. Hou, M. Du, R. H. Zhang, F. Brisse, *Inorg. Chem.* 41 (2002) 3477.

- [12] (a) M. L. Han, X. H. Chang, X. Feng, L. F. Ma, L. Y. Wang, *CrystEngComm* 16 (2014) 1687; (b) D. C. Zhong, W. G. Lu, J. H. Deng, *CrystEngComm* 16 (2014) 4633.
- [13] (a) Y. B. Go, X. Wang, E. V. Anokhina, A. J. Jacobson, *Inorg. Chem.* 44 (2005) 8265; (b) J. H. Wang, G. M. Tang, Y. T. Wang, T. X. Qin, S. W. Ng, *CrystEngComm* 16 (2014) 2660; (c) L. Cheng, J. Wang, Q. Qi, X. Zhang, H. Yu, S. Gou, L. Fang, *CrystEngComm* 16 (2014) 10056.
- [14] P. M. Forster, N. Stock, A. K. Cheetham, *Angew. Chem. Int. Ed.* 44 (2005) 7608.
- [15] (a) B. Chen, L. Wang, Y. Xiao, F. R. Fronczek, M. Xue, Y. Cui, G. Qian, *Angew. Chem. Int. Ed.* 48 (2009) 500; (b) T. Li, X. Liu, Z.-P. Huang, Q. Lin, C.-L. Lin, Q.-G. Zhan, X.-D. Xu, Y.-P. Cai, *Inorg. Chem. Commun.* 39 (2014) 70; (c) Y. T. Wang, G. M. Tang, Z. W. Qiang, *Polyhedron* 26 (2007) 4542; (d) Y. T. Wang, T. X. Qin, C. Zhao, G. M. Tang, T. D. Li, Y. Z. Cui, J. Y. Li, *J. Mol. Struct.* 938 (2009) 291.
- [16] (a) B. H. Ye, M. L. Tong, X. M. Chen, *Coord. Chem. Rev.* 249 (2005) 545; (b) Y.-Z. Zheng, Z. Zheng, X.-M. Chen, *Coord. Chem. Rev.* 258–259 (2014) 1; (c) N. N. Adarsh, P. Dastidar, *Chem. Soc. Rev.* 41 (2012) 3039; (d) F. A. Almeida Paz, J. Klinowski, S. M. F. Vilela, J. P. C. Tome, J. A. S. Cavaleiro, J. Rocha, *Chem. Soc. Rev.* (2012) 1088; (e) Y. He, B. Li, M. O'Keeffe, B. Chen, *Chem. Soc. Rev.* 43 (2014) 5618; (f) S. Kitagawa, K. Uemura, *Chem. Soc. Rev.* 34 (2005) 109; (g) F. A. A. Paz, J. Klinowski, S. M. F. Vilela, J. P. C. Tome, J. A. S. Cavaleiro, J. Rocha, *Chem. Soc. Rev.* 41 (2012) 1088; (h) Q. L. Zhu, Q. Xu, *Chem. Soc. Rev.* 43 (2014) 5468; (i) H.-L. Jiang, T. A. Makal, H.-C. Zhou, *Coord. Chem. Rev.* 257 (2013) 2232; (j) C. Pettinari, A. Tăbăcaru, S. Galli, *Coord. Chem. Rev.* 307, Part 1 (2016) 1; (k) C. B. Aakeroy, N. R. Champness, C. Janiak, *CrystEngComm* 12 (2010) 22.
- [17] (a) L. P. Zhang, J. F. Ma, J. Yang, Y. Y. Pang, J. C. Ma, *Inorg. Chem.* 49 (2010) 1535; (b) Y. G. Ran, J. X. Xie, Y. J. Mu, L. F. Zhang, B. Han, *Inorg. Chim. Acta* 425 (2015) 17; (c) S. Y. Zhang, Z. J. Zhang, W. Shi, B. Zhao, P. Cheng, *Inorg. Chim. Acta* 363 (2010) 3784; (d) Y. Yan, C. D. Wu, X. He, Y. Q. Sun, C. Z. Lu, *Cryst. Growth Des.* 5 (2005) 821; (e) J.-H. Wang, G.-M. Tang, T.-X. Qin, S.-C. Yan, Y.-T. Wang, Y.-Z. Cui, S. Weng Ng, *J. Solid State Chem.* 219 (2014) 55; (f) Y.-Q. Zheng, H.-L. Zhu, J.-L. Lin, W. Xu, F.-H. Hu, *J. Solid State Chem.* 201 (2013) 1; (g) L. Cheng, J. Wang, H.-Y. Yu, X.-Y. Zhang, S.-H. Gou, L. Fang, *J. Solid State Chem.* 221 (2015) 85.
- [18] (a) C. Ding, X. Rui, C. Wang, Y. Xie, *CrystEngComm* 16 (2014) 1010; (b) H. S. Wang, W. Shi, J. Xia, H. B. Song, H. G. Wang, P. Cheng, *Inorg. Chem. Commun.* 10 (2007) 856; (c) W. Sun, J. Liu, H. Liu, Z. Liu, *Polyhedron* 109 (2016) 1.
- [19] (a) Y. H. Zhou, *J. Inorg. Organomet. Polym.* 23 (2013) 1189; (b) C.-C. Wang, J.-H. Wang, G.-M. Tang, Y.-T. Wang, Y.-Z. Cui, S. W. Ng, *J. Coord. Chem.* 68 (2015) 3918; (c) Y. T. Wang, G. M. Tang, *J. Coord. Chem.* 60 (2007) 2139; (d) Y. T. Wang, G. M. Tang, Y. C. Zhang, W. Z. Wan, J. C. Yu, T. D. Li, Y. Z. Cui, *J. Coord. Chem.* 63 (2010) 1504; (e) Y. T. Wang, W. Z. Wan, G. M. Tang, Z. W. Qiang, T. D. Li, *J. Coord. Chem.* 63 (2010) 206.
- [20] (a) Y. Yang, M. H. Zeng, L. J. Zhang, H. Liang, *J. Coord. Chem.* 62 (2009) 886; (b) C. K. Xia, C. Z. Lu, X. Y. Wu, Q. Z. Zhang, H. J. Zhang, D. M. Wu, *Polyhedron* 26 (2007) 941; (c) N. Kundu, A. Audhya, S. M. T. Abtab, S. Ghosh, E. R. T. Tiekink, M. Chaudhury, *Cryst. Growth Des.* 10 (2010) 1269; (d) C. J. Wang, K. F. Yue, Z. X. Tu, L. L. Xu, Y. L. Liu, Y. Y. Wang, *Cryst. Growth Des.* 11 (2011) 2897; (e) M. X. Li, H. Wang, S. W. Liang, M. Shao, X. He, Z. X. Wang, S. R. Zhu, *Cryst. Growth Des.* 9 (2009) 4626; (f) X. P. Li, M. Pan, S. R. Zheng, Y. R. Liu, Q. T. He, B. S. Kang, C. Y. Su, *Cryst. Growth Des.* 7 (2007) 2481; (g) H. Wang, M. X. Li, M. Shao, X. He, *Polyhedron* 26 (2007) 5171; (h) F. Li, Y. Kang, Y. M. Dai, J. A. Zhang, *Inorg. Chem. Commun.* 14 (2011) 228; (i) T. Lu, X. Xu, H. Li, Z. Li, X. Zhang, J. Ou, M. Mei, *Dalton Trans.* 44 (2015) 2267; (j) I. Elguraish, K. Zhu, L. A. Hernandez, H. Amarne, J. Luo, V. N. Vukotic, S. J. Loeb, *Dalton Trans.* 44 (2015) 898; (k) C. K. Xia, C. Z. Lu, X. Y. Wu, L. J. Chen, Q. Z. Zhang, J. J. Zhang, D. M. Wu, *Inorg. Chim. Acta* 359 (2006) 4639; (l) L. J. Chen, X. He, C. K. Xia, Q. Z. Zhang, J. T. Chen, W. B. Yang, C. Z. Lu, *Cryst. Growth Des.* 6 (2006) 2076; (m) C. K. Xia, C. Z. Lu, Q. Z. Zhang, X. He, J. J. Zhang, D. M. Wu, *Cryst. Growth Des.* 5 (2005) 1569.

- [21] M. Allegretti, R. Bertini, M. C. Cesta, C. Bizzarri, R. D. Bitondo, V. D. Cioccio, E. Galliera, V. Berdini, A. Topai, G. Zampella, V. Russo, N. D. Bello, G. Nano, L. Nicolini, M. Locati, P. Fantucci, Saverio Florio, F. Colotta, *J. Med. Chem.* 48 (2005) 4312.
- [22] S. Park, J. Jung, E. J. Cho, *Eur. J. Org. Chem.* 2014 (2014) 4148.
- [23] S. Y. Lin, Y. Isome, E. Stewart, J. F. Liu, D. Yohannes, L. B. Yu, *Tetrahedron Lett.* 47 (2006) 2883.
- [24] CrysAlisPro, Oxford Diffraction Poland (2009).
- [25] Bruker, AXS, SAINT Software Reference Manual; Madison: WI (1998).
- [26] (a) G. M. Sheldrick, SHELXTL NT Version 5.1. Program for Solution and Refinement of Crystal Structures; University of Göttingen: Germany (1997); (b) G. M. Sheldrick, *Acta Crystallogr. Sect. A* 64 (2008) 112.
- [27] A. L. Spek, *J. Appl. Cryst.* 36 (2003) 7.
- [28] T. Mathavan, S. Umapathy, M. A. Jothirajan, A. M. F. Benial, *Spectrosc. Lett.* 45 (2012) 588.
- [29] (a) B. K. Das, S. J. Bora, M. Chakraborty, L. Kalita, R. Chakrabarty, R. Barman, *J. Chem. Sci.* 118 (2006) 487; (b) E. Viñuelas-Zahínos, M. A. Maldonado-Rogado, F. Luna-Giles, F. J. Barros-García, *Polyhedron* 27 (2008) 879.
- [30] (a) M. A. Maldonado-Rogado, E. Viñuelas-Zahínos, F. Luna-Giles, F. J. Barros-García, *Polyhedron* 26 (2007) 5210; (b) F. J. Barros-García, A. Bernalte-García, F. Luna-Giles, M. A. Maldonado-Rogado, E. Viñuelas-Zahínos, *Polyhedron* 25 (2006) 52; (c) E. Viñuelas-Zahínos, F. Luna-Giles, P. Torres-García, A. Bernalte-García, *Polyhedron* 28 (2009) 4056.
- [31] M. V. Angelusiu, S. F. Barbuceanu, C. Draghici, G. L. Almajan, *Eur. J. Med. Chem.* 45 (2010) 2055.
- [32] X.-M. Chen, J.-W. Cai, *Single-Crystal Structural Analysis Principles and Practices*; the Science Press: Beijing (2003).
- [33] D. Sun, L. L. Han, S. Yuan, Y. K. Deng, M. Z. Xu, D. F. Sun, *Cryst. Growth Des.* 13 (2013) 377.
- [34] (a) Z. Su, J. Fan, T.-a. Okamura, W. Y. Sun, N. Ueyama, *Cryst. Growth Des.* 10 (2010) 3515; (b) H. Furukawa, N. Ko, Y. B. Go, N. Aratani, S. B. Choi, E. Choi, A. O. Yazaydin, R. Q. Snurr, M. O'Keeffe, J. Kim, O. M. Yaghi, *Science* 329 (2010) 424.
- [35] A. C. Tella, S. O. Owolude, *J. Mater. Sci.* 49 (2014) 5635.
- [36] (a) X. L. Wang, J. Luan, H. Y. Lin, M. Le, G. C. Liu, *Dalton Trans.* 43 (2014) 8072; (b) H. Wu, W. J. Sun, T. Shi, X. Z. Liao, W. J. Zhao, X. Yang, *CrystEngComm* 16 (2014) 11088.
- [37] Y. Gong, J. Li, J. Qin, T. Wu, R. Cao, J. Li, *Cryst. Growth Des.* 11 (2011) 1662.
- [38] (a) M. Xue, G. S. Zhu, Q. R. Fang, X. D. Guo, S. L. Qiu, *Inorg. Chem. Commun.* 9 (2006) 603; (b) B. Valeur, *Molecular Fluorescence Principles and Applications*; WILEY-VCH: Weinheim (2002).



**Scheme 1.** Structures of  $H_2L$  and  $4PBI$  ligands



**Scheme 2.** The coordination modes for ligand  $L$  (a,b) and  $4PBI$  (c,d)

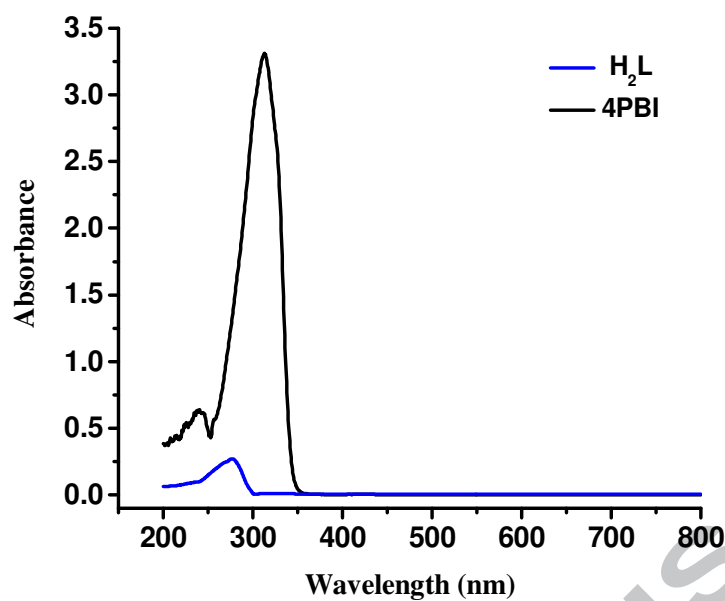


Fig. 1. UV-Visible absorbance spectra of the free ligands **H<sub>2</sub>L** and **4PBI** in DMF solution.

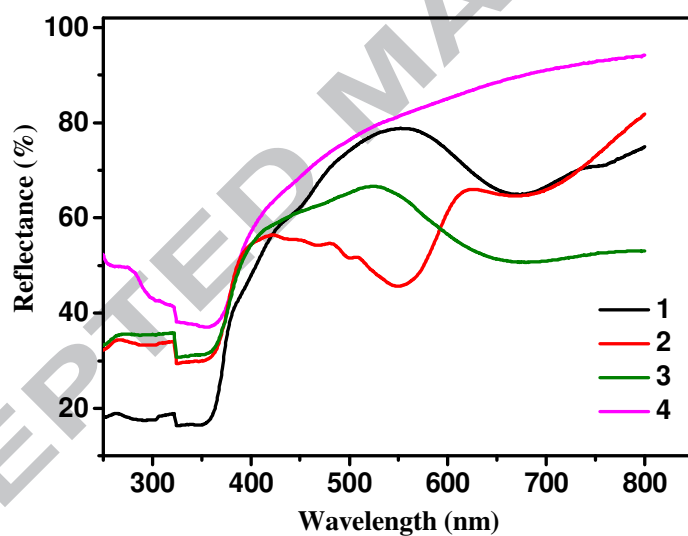
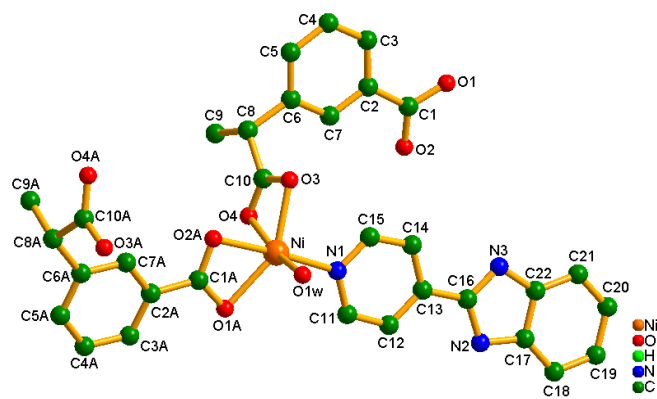
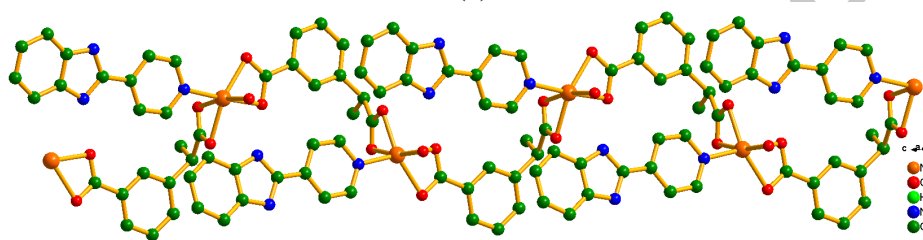


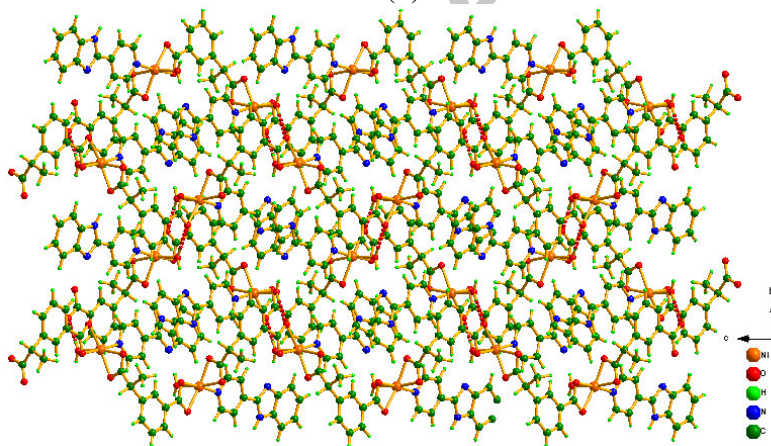
Fig. 2. UV-Visible diffuse reflectance spectra of complexes **1-4** in solid state.



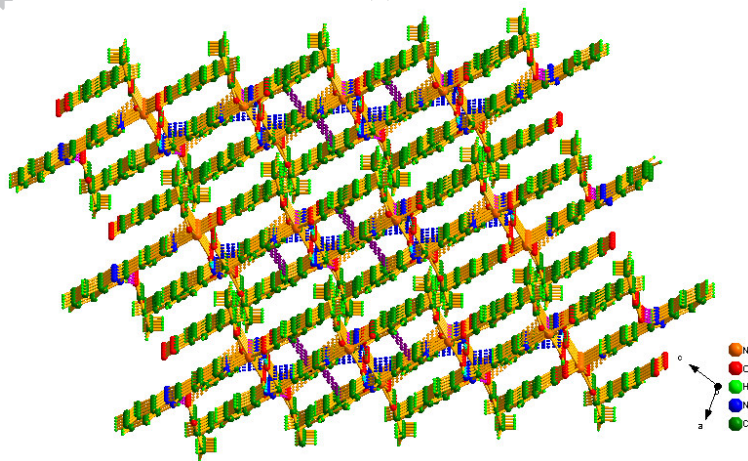
(a)



(b)

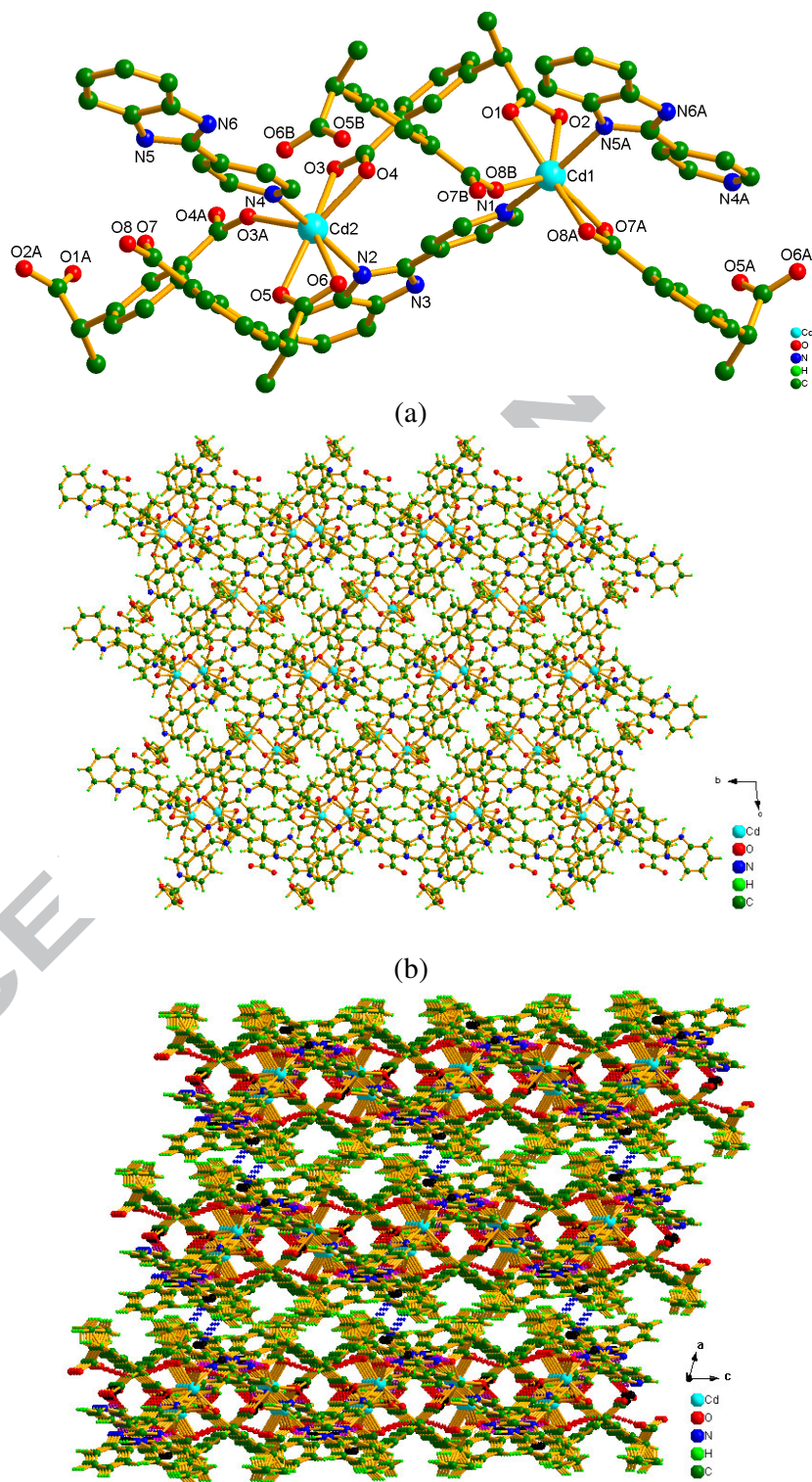


(c)



(d)

Fig. 3. (a) A perspective view of the coordination geometry of the Ni (II) centre in **1**. (b) A 1D chain along the *c* axis in **1**. (c) A 2D supramolecular network formed by hydrogen bond interactions in **1**. (d) The packing diagram of **1** along the *b* axis



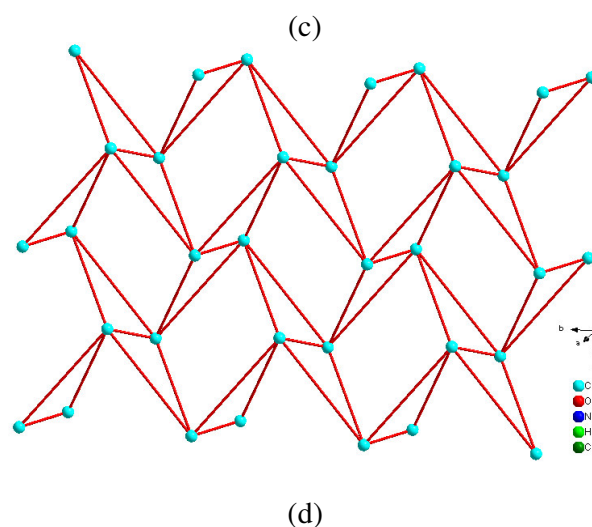


Fig. 4. (a) A perspective view of the coordination geometry of the Cd centre in **4** and the bis-nucleic structure in **4**. (b) A 2D layer along the crystallographic *bc* plane. (c) The packing diagram of **4**. (d) The topology structure of **4**.

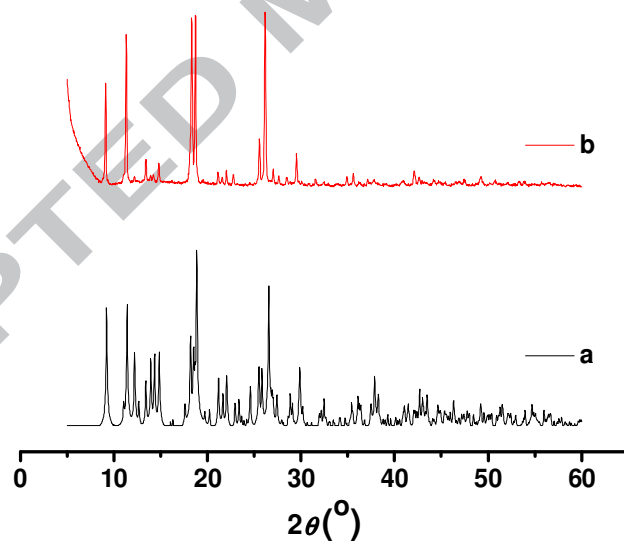


Fig. 5. Powder X-ray diffraction (PXRD) plots for **1**. (a) simulated; (b) experimental

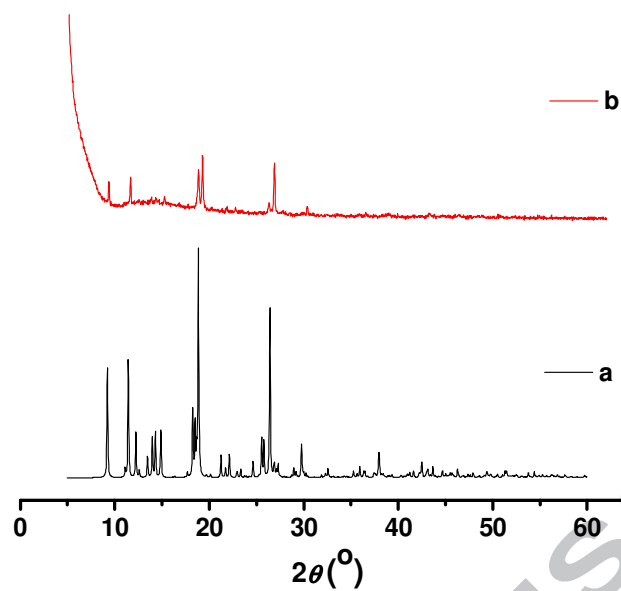


Fig. 6. PXRd plots for **2**. (a) simulated; (b) experimental

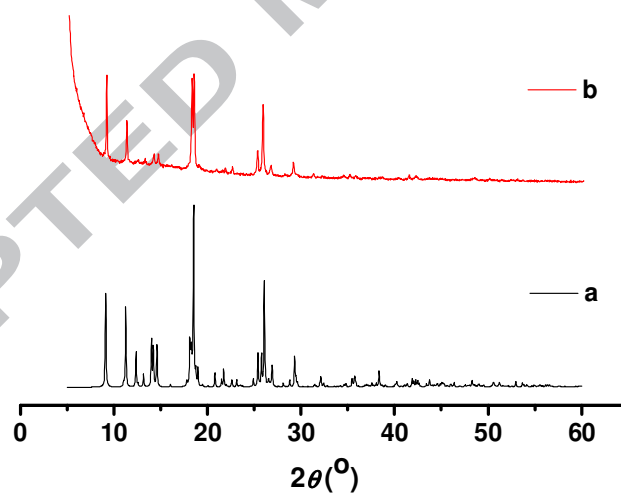


Fig. 7. PXRd plots for **3**. (a) simulated; (b) experimental

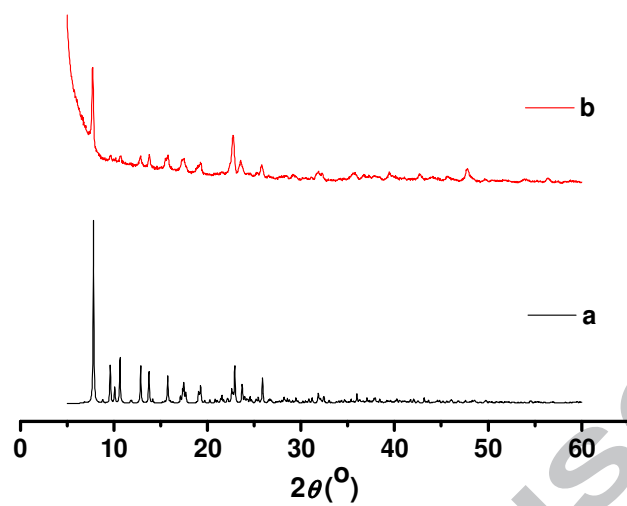


Fig. 8. PXRD plots for **4**. (a) simulated; (b) experimental

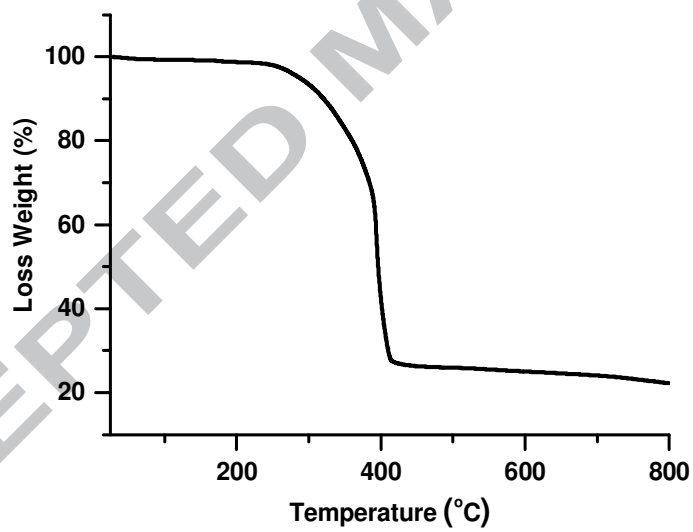


Fig. 9. TGA curve of **1**.

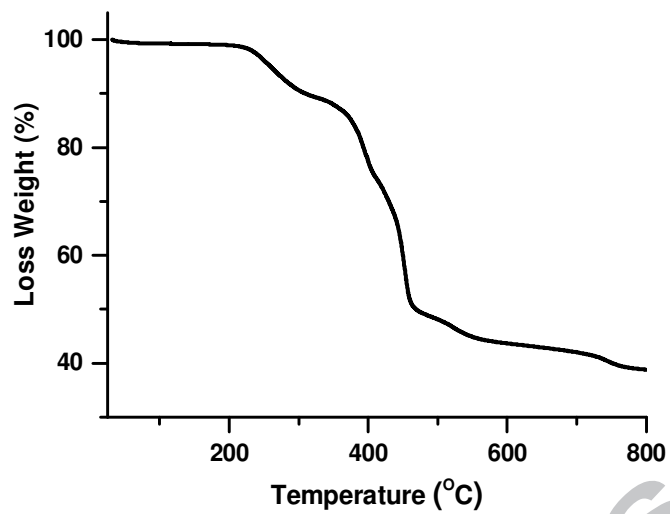


Fig. 10. TGA curve of 2.

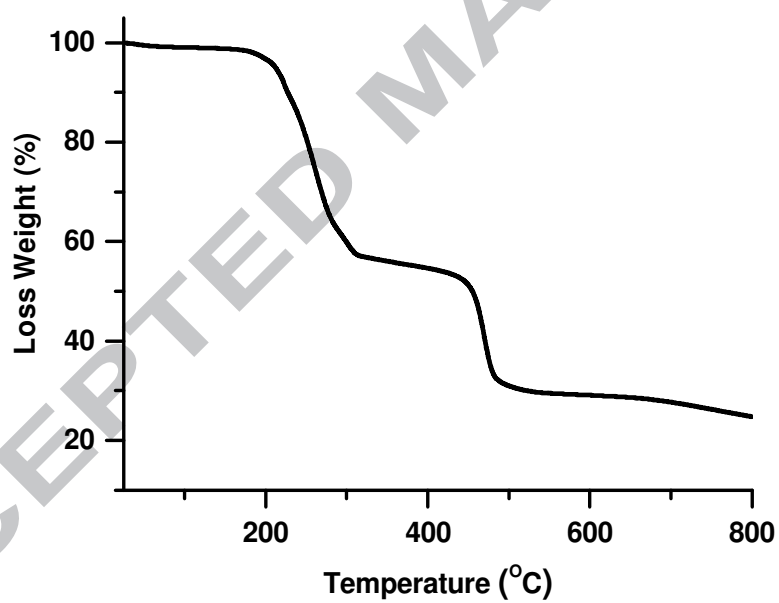


Fig. 11. TGA curve of 3.

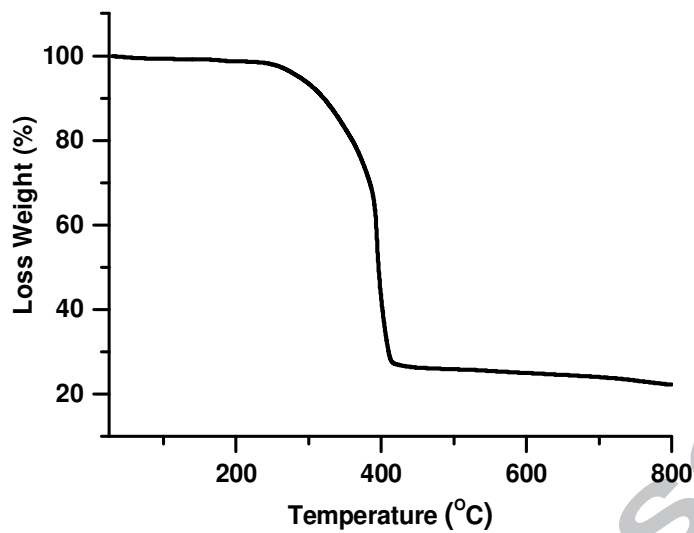


Fig. 12. TGA curve of **4**.

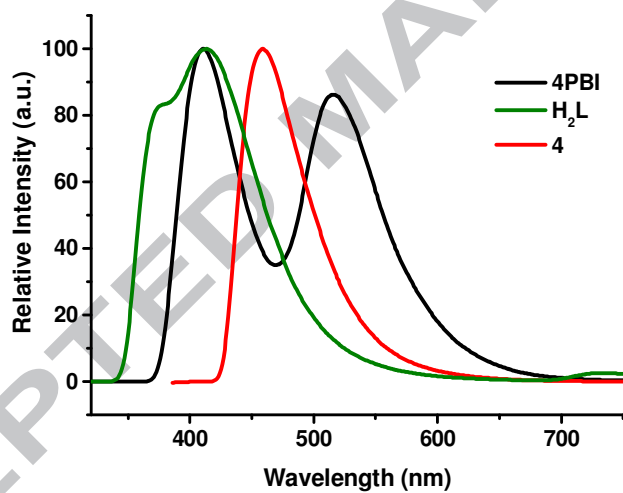


Fig. 13. The solid-state emission spectra of complex **4**, **4PBI** and **H<sub>2</sub>L** ligand.

**Table 1.** The UV–Vis spectral data of **H<sub>2</sub>L** and **4PBI**

Compound	A	C (10 <sup>-4</sup> ) (M)	$\lambda_{\max}$ (nm)	lg $\epsilon$	Solvent
<b>L</b>	0.27	2.78	278	4.98	DMF
<b>4PBI</b>	3.31	1.84	314	6.25	DMF

**Table 2.** Crystal data and structure refinement data for **1-4**

Compound reference	<b>1</b>	<b>2</b>	<b>3</b>	<b>4</b>
Chemical formula	C <sub>22</sub> H <sub>19</sub> N <sub>3</sub> NiO <sub>5</sub>	C <sub>22</sub> H <sub>19</sub> CoN <sub>3</sub> O <sub>5</sub>	C <sub>22</sub> H <sub>19</sub> CuN <sub>3</sub> O <sub>5</sub>	C <sub>22</sub> H <sub>17</sub> CdN <sub>3</sub> O <sub>4</sub>
Formula Mass	464.11	464.33	468.94	499.79
Crystal system	Monoclinic	Monoclinic	Monoclinic	Triclinic
<i>a</i> /Å	10.5053(7)	10.4737(7)	10.4805(9)	12.5721(5)
<i>b</i> /Å	13.1794(7)	13.1355(6)	13.4316(8)	2.6827(4)
<i>c</i> /Å	14.5680(8)	14.6668(8)	14.7788(13)	13.4256(6)
$\alpha$ /°	90.00	90.00	90.00	89.999(3)
$\beta$ /°	106.672(7)	106.884(7)	108.109(10)	74.554(4)
$\gamma$ /°	90.00	90.00	90.00	69.597(4)
Unit cell volume/Å <sup>3</sup>	1932.2(2)	1930.84(19)	1977.4(3)	1923.69(13)
Temperature/K	100(2)	100(2)	100(2)	100(2)
Space group	<i>P</i> 2 <sub>1</sub> / <i>n</i>	<i>P</i> 2 <sub>1</sub> / <i>n</i>	<i>P</i> 2 <sub>1</sub> / <i>n</i>	<i>P</i> -1
No. of formula units per unit cell, <i>Z</i>	4	4	4	4
Radiation type	Mo K $\alpha$	Mo K $\alpha$	Mo K $\alpha$	Mo K $\alpha$
Absorption coefficient, $\mu$ /mm <sup>-1</sup>	1.047	0.931	1.146	1.171
No. of reflections measured	17712	17462	19536	18605
No. of independent reflections	4461	4474	4574	8887
<i>R</i> <sub>int</sub>	0.0485	0.0486	0.0596	0.0430
Final <i>R</i> <sub>i</sub> values ( <i>I</i> >2 $\sigma$ ( <i>I</i> )) <sup>a</sup>	0.0486	0.0432	0.0526	0.0409
Final <i>wR</i> ( <i>F</i> <sup>2</sup> ) values ( <i>I</i> >2 $\sigma$ ( <i>I</i> ))	0.1170	0.1154	0.1298	0.0843
Final <i>R</i> <sub>i</sub> values (all data)	0.0584	0.0571	0.0776	0.0628
Final <i>wR</i> ( <i>F</i> <sup>2</sup> ) values (all data) <sup>b</sup>	0.1237	0.1285	0.1470	0.0978
Goodness of fit on <i>F</i> <sup>2</sup>	1.075	1.023	1.036	1.040
CCDC number	994678	994679	994680	994681

<sup>a</sup> $R_1 = \sum |F_o| - |F_c| / \sum |F_o|$ , <sup>b</sup> $wR_2 = [\sum [w(F_o^2 - F_c^2)^2] / \sum [w(F_o^2)^2]]^{1/2}$ .

**Table 3.** Selected bond lengths (Å) and angles (°) for complexes **1-4**.

<b>1</b>			
Ni(1)-O(1)	2.154(2)	Ni(1)-O(1W)	2.033(2)
Ni(1)-O(2)	2.057(2)	Ni(1)-N(1)	2.058(2)
Ni(1)-O(3) <sup>a</sup>	2.106(2)	Ni(1)-O(4) <sup>a</sup>	2.132(2)
O(1)-Ni(1)-O(1W)	89.17(8)	O(1)-Ni(1)-O(2)	62.85(8)
O(1)-Ni(1)-N(1)	113.41(9)	O(1)-Ni(1)-O(3) <sup>a</sup>	148.07(8)
O(1)-Ni(1)-O(4) <sup>a</sup>	98.30(8)	O(1W)-Ni(1)-O(2)	88.43(8)
O(1W)-Ni(1)-N(1)	92.36(9)	O(1W)-Ni(1)-O(3) <sup>a</sup>	107.15(8)
O(1W)-Ni(1)-O(4) <sup>a</sup>	168.50(8)	O(2)-Ni(1)-N(1)	176.17(9)
O(2)-Ni(1)-O(3) <sup>a</sup>	89.75(8)	O(2)-Ni(1)-O(4) <sup>a</sup>	87.25(8)
N(1)-Ni(1)-O(3) <sup>a</sup>	93.60(9)	N(1)-Ni(1)-O(4) <sup>a</sup>	92.67(8)
O(3) <sup>a</sup> -Ni(1)-O(4) <sup>a</sup>	62.20(8)		
<b>2</b>			
Co(1)-O(1)	2.1957(18)	Co(1)-O(1W)	2.045(2)
Co(1)-O(2)	2.0940(19)	Co(1)-N(1)	2.099(2)
Co(1)-O(3) <sup>a</sup>	2.1407(17)	Co(1)-O(4) <sup>a</sup>	2.1675(18)
O(1)-Co(1)-O(1W)	89.68(7)	O(1)-Co(1)-O(2)	61.41(7)
O(1)-Co(1)-N(1)	114.42(7)	O(1W)-Co(1)-O(2)	89.55(8)
O(1)-Co(1)-O(3) <sup>a</sup>	145.81(7)	O(1)-Co(1)-O(4) <sup>a</sup>	97.99(7)
O(1W)-Co(1)-N(1)	92.55(8)	O(1W)-Co(1)-O(3) <sup>a</sup>	108.52(7)
O(1W)-Co(1)-O(4) <sup>a</sup>	169.03(7)	O(2)-Co(1)-O(4) <sup>a</sup>	87.28(7)

O(2)-Co(1)-N(1)	175.35(8)	O(2)-Co(1)-O(3) <sup>a</sup>	89.29(7)
N(1)-Co(1)-O(3) <sup>a</sup>	93.98(8)	N(1)-Co(1)-O(4) <sup>a</sup>	91.40(8)
O(3)b-Co(1)-O(4) <sup>a</sup>	60.97(7)		
<b>3</b>			
Cu(1)-O(1)	2.464(2)	Cu(1)-O(1W)	1.972(3)
Cu(1)-O(2)	1.973(2)	Cu(1)-N(1)	1.994(3)
Cu(1)-O(3) <sup>a</sup>	2.398(2)	Cu(1)-O(4) <sup>a</sup>	2.024(2)
O(1)-Cu(1)-O(1W)	89.75(9)	O(1)-Cu(1)-O(2)	58.50(8)
O(1)-Cu(1)-N(1)	113.56(10)	O(1W)-Cu(1)-O(2)	89.40(11)
O(1)-Cu(1)-O(3) <sup>a</sup>	145.45(8)	O(1)-Cu(1)-O(4) <sup>a</sup>	101.01(9)
O(1W)-Cu(1)-N(1)	92.49(12)	O(1W)-Cu(1)-O(3) <sup>a</sup>	107.23(9)
O(1W)-Cu(1)-O(4) <sup>a</sup>	166.00(10)	O(2)-Cu(1)-O(4) <sup>a</sup>	88.65(9)
O(2)-Cu(1)-N(1)	171.85(10)	O(2)-Cu(1)-O(3) <sup>a</sup>	91.06(8)
N(1)-Cu(1)-O(3) <sup>a</sup>	95.95(10)	N(1)-Cu(1)-O(4) <sup>a</sup>	91.38(11)
O(3) <sup>c</sup> -Cu(1)-O(4) <sup>a</sup>	58.96(8)		
<b>4</b>			
Cd1-O1	2.251(3)	Cd1-N1	2.328(3)
Cd1-O7 <sup>a</sup>	2.353(3)	Cd1-O8 <sup>a</sup>	2.459(3)
Cd1-N5 <sup>a</sup>	2.360(3)	Cd1-O8 <sup>c</sup>	2.360(2)
Cd2-O3	2.481(3)	Cd2-O4	2.349(3)
Cd2-O5	2.267(3)	Cd2-N2	2.359(4)
Cd2-N4	2.318(4)	Cd2-O3 <sup>d</sup>	2.354(2)
O1-Cd1-N1	85.84(12)	O1-Cd1-O7 <sup>a</sup>	148.61(9)
O1-Cd1-O8 <sup>b</sup>	155.83(8)	N1-Cd1-O7 <sup>b</sup>	83.43(11)
O1-Cd1-N5 <sup>b</sup>	86.70(12)	O1-Cd1-O8 <sup>c</sup>	87.31(9)
N1-Cd1-O8 <sup>b</sup>	109.76(12)	N1-Cd1-N5 <sup>b</sup>	163.86(12)
N1-Cd1-O8 <sup>c</sup>	89.34(10)	O7 <sup>b</sup> -Cd1-O8 <sup>c</sup>	121.87(9)
O7 <sup>b</sup> -Cd1-O8 <sup>b</sup>	54.48(8)	O7 <sup>b</sup> -Cd1-N5 <sup>b</sup>	95.69(11)
O8 <sup>b</sup> -Cd1-N5 <sup>b</sup>	82.19(11)	O8 <sup>b</sup> -Cd1-O8 <sup>c</sup>	74.93(9)
N5 <sup>b</sup> -Cd1-O8 <sup>a</sup>	104.59(10)	O3-Cd2-N2	83.27(11)
O3-Cd2-O4	54.26(8)	O3-Cd2-O5	157.12(8)
O3-Cd2-N4	108.61(11)	O3-Cd2-O3 <sup>d</sup>	74.25(8)
O4-Cd2-O5	147.56(9)	O4-Cd2-O3 <sup>d</sup>	121.48(9)
O4-Cd2-N2	95.75(9)	O4-Cd2-N4	84.06(9)
O5-Cd2-N2	86.33(11)	O5-Cd2-N4	85.71(11)
O5-Cd2-O3 <sup>d</sup>	88.84(9)	N4-Cd2-O3 <sup>d</sup>	88.39(10)
N2-Cd2-N4	164.60(13)	N2-Cd2-O3 <sup>d</sup>	104.62(10)

Symmetry codes: <sup>a</sup>1/2+x,1/2-y,1/2+z. <sup>b</sup>x,y,-1+z. <sup>c</sup>1-x,1-y,1-z. <sup>d</sup>1-x,2-y,1-z.

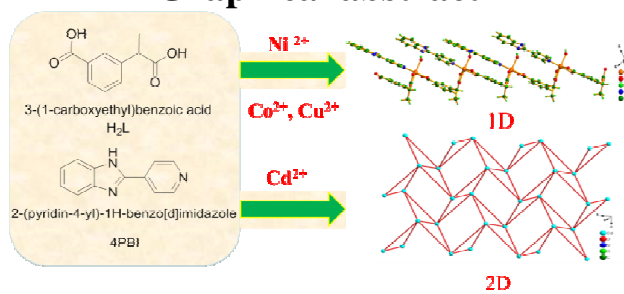
**Table 4.** Hydrogen bond geometries in the crystal structure of **1-4**, respectively.

Compound	D-H...A <sup>a</sup>	H...A (Å)	D...A (Å)	D-H...A (°)
<b>1</b>	N(2)-H(2)...O(3) <sup>a</sup>	1.84(2)	2.713(3)	170(4)
	O(1W)-H(11)...O(1) <sup>a</sup>	1.92(3)	2.743(3)	168(3)
	O(1W)-H(12)...N(3) <sup>b</sup>	1.88(2)	2.719(3)	170(4)
	C(5)-H(5)...O(4) <sup>c</sup>	2.58	3.361(4)	140
	C(14)-H(14)...O(1W) <sup>d</sup>	2.60	3.487(4)	156
	C(15)-H(15)...O(3) <sup>d</sup>	2.35	2.991(4)	125
<b>2</b>	N(2)-H(2)...O(3) <sup>a</sup>	1.83(2)	2.706(3)	171(3)
	O(1W)-H(11)...O(1) <sup>a</sup>	1.88(3)	2.709(3)	167(3)
	O(1W)-H(12)...N(3) <sup>b</sup>	1.87(2)	2.697(3)	170(3)
	C(5)-H(5)...O(4) <sup>c</sup>	2.55	3.330(3)	139
	C(12)-H(12A)...O(3) <sup>a</sup>	2.54	3.451(3)	160
	C(14)-H(14)...O(1W) <sup>d</sup>	2.57	3.465(3)	157
	C(15)-H(15)...O(3) <sup>d</sup>	2.40	3.053(4)	126
<b>3</b>	N(2)-H(2)...O(3) <sup>a</sup>	1.81(3)	2.688(3)	176(3)
	O(1W)-H(11)...O(1) <sup>a</sup>	1.80(3)	2.636(3)	174(4)
	O(1W)-H(12)...N(3) <sup>b</sup>	1.86(2)	2.695(4)	175(5)
	C(12)-H(12A)...O(3) <sup>a</sup>	2.54	3.451(4)	160

4	C(14)–H(14)···O(1W) <sup>d</sup>	2.53	3.441(5)	160
	C(15)–H(15)···O(3) <sup>d</sup>	2.48	3.175(5)	130
	N3–H3···O2 <sup>e</sup>	1.92	2.737(4)	153
	N6–H6···O6 <sup>a</sup>	1.94	2.734(5)	149
	C7–H7···O5 <sup>f</sup>	2.49	3.204(5)	132
	C17–H17···O1 <sup>a</sup>	2.51	3.201(5)	130
	C21–H21···O8 <sup>a</sup>	2.45	3.164(5)	132
	C22–H22···O6	2.36	3.296(5)	168
	C24–H24···O2 <sup>e</sup>	2.57	3.469(4)	157
	C33–H33···O3 <sup>f</sup>	2.42	3.134(5)	131
	C34–H34···O2 <sup>g</sup>	2.34	3.274(4)	169
	C36–H36···O6 <sup>a</sup>	2.58	3.480(4)	158

Symmetry codes: <sup>a</sup>1-x, 1-y, 1-z. <sup>b</sup>-1/2+x, 1/2-y, -1/2+z. <sup>c</sup>-1/2-x, 1/2+y, 1/2-z. <sup>d</sup>1/2+x, 1/2-y, 1/2+z. <sup>e</sup>1-x, 2-y, -z. <sup>f</sup>1-x, 2-y, 1-z. <sup>g</sup>x, y, 1+z

## Graphical abstract



A set of metal coordination polymers with different motifs have been obtained, which are constructed by a novel semi-rigid aromatic carboxylate ligand under hydrothermal reaction conditions. The Cd-based complex displays interesting luminescent property.

ACCEPTED MANUSCRIPT